

PREPARED FOR SUBMISSION TO JINST

EUROPEAN INSTITUTE FOR MOLECULAR IMAGING

JUNE 2022

UNIVERSITY OF MÜNSTER

Suppression of electrical breakdown phenomena in liquid TriMethyl Bismuth based ionization detectors

Björn Gerke,¹ Simon-Nis Peters,² Nils Marquardt,² Christian Huhmann,² Volker Michael Hannen,² Michael Holtkamp,³ Uwe Karst,³ Dominique Yvon,^{4,5} Viatcheslav Sharyy,^{4,5} Christian Weinheimer,² Klaus Schäfers¹

¹*European Institute for Molecular Imaging, University of Münster, Münster, Germany*

²*Institute for Nuclear Physics, University of Münster, Münster, Germany*

³*Institute of Inorganic and Analytical Chemistry, University of Münster, Münster, Germany*

⁴*IRFU, CEA, Université Paris-Saclay, Gif-sur-Yvette, France*

⁵*BioMAPs, Service Hospitalier Frédéric Joliot, CEA, CNRS, Inserm, Université Paris-Saclay, Orsay, France*

E-mail: gerkeb@uni-muenster.de

ABSTRACT:

Organometallic liquids provide good properties for ionization detectors. TriMethyl Bismuth (TMBi) has been proposed as a detector medium with charge and Cherenkov photon readout for Positron Emission Tomography. In this work, we present studies for the handling of TMBi at different electric fields and under different environmental conditions to find applicable configurations for the suppression of electrical breakdowns in TMBi at room temperature. A simple glass cell with two electrodes filled with TMBi was constructed and tested under different operation conditions. Working at the vapour pressure of TMBi at room temperature of about 40 mbar and electric fields of up to 20 kV/cm in presence of a small oxygen contamination we found the formation of a discharge channel in the liquid and a steady increase in the current. Further reduction of pressure by pumping caused the TMBi to boil and a spontaneous combustion. Eliminating the oxygen contamination led the TMBi under the same condition to only decompose. When operating the setup under an argon atmosphere of 1 bar we did not observe breakdowns of the electrical potential up to field strengths of 20 kV/cm. Still, in presence of a small oxygen contamination fluctuating currents in the nA range were observed, but no decomposition or combustion. We conclude from our experiments that TMBi at room temperature in a pure argon atmosphere of 1 bar remains stable against electrical breakdown at least up to electric field strengths of 20 kV/cm, presumably because the formation of gaseous TMBi was prevented.

KEYWORDS: liquid detectors, gamma detectors

¹Corresponding author.

Contents

1	Introduction	1
2	Electrical breakdown phenomena	2
2.1	Electrical breakdown in gases	2
2.2	Electrical breakdown in dielectric liquids	3
2.3	Electrical breakdown behavior of TMBi	4
3	Setup for breakdown experiments	5
4	Measurement results	6
4.1	Experiment 1: 1 bar argon atmosphere and oxygen contamination.	6
4.2	Experiment 2: vapor pressure (40 mbar) and oxygen contamination.	7
4.3	Experiment 3: low pressure (< 40 mbar) and oxygen contamination	7
4.4	Experiment 4: low pressure argon atmosphere	9
4.5	Experiment 5: 1 bar argon atmosphere	9
5	Conclusion	10

1 Introduction

Liquid ionization detectors have been proposed for many applications both in low energy particle physics as well as medical imaging [1][2][3]. Noble element liquid detectors, e.g. based on argon or xenon, offer a promising combination of excellent scintillation properties in conjunction with the capability to drift charges [4]. They find application in large-scale dark matter [5][6][7][8][9] and neutrinoless double beta decay experiments [10][11]. While liquid xenon is a very effective detector material with high density (5.9 g/cm^3) and high Z (54), cryogenic temperatures are required for operation, as has been reported for its use in a time projection chamber ($-96 \text{ }^\circ\text{C}$ at 1.935 bar) [12]. This is of some limitation for such a detector system if it would be used in a medical environment. Nevertheless, new detector concepts for positron emission tomography (PET) have been introduced recently based on liquid xenon detectors with the advantage of providing large area detectors [13][14]. This is of special interest in whole-body sized PET scanners for simplifying the detector setup which is commonly built on thousands of small pixelated detector elements.

With the idea of operating at room temperature, a new drift detector has been proposed for PET based on an heavy organometallic liquid - TriMethyl Bismuth (TMBi) [15][16]. TMBi (chemical formula $(\text{CH}_3)_3\text{Bi}$) is a transparent dielectric liquid consisting of three methyl groups and one bismuth atom. Because of the high atomic number of bismuth ($Z_{\text{Bi}} = 83$) TMBi effectively converts 511 keV photons by the photo-electric effect (47 % photo fraction) offering the possibility to read

out both charges in a high resolution drift detector as well as Cherenkov light of the primary photoelectron for fast event timing. High electric field strengths are required to separate electron-ion pairs generated in the liquid and to drift the electrons towards a segmented anode. The liquid must be highly purified to reduce recombination [17][18]. However, high field strengths can trigger an electric breakdown in the liquid generating high local temperatures. Temperatures above 106 °C lead to a decomposition of TMBi resulting in a sudden increase in volume. Such an event happened recently at *IRFU, CEA, Université Paris-Saclay* causing an unexpected explosion during an experiment [19].

In this work we present test measurements regarding the handling of TMBi at different electric fields and under different environmental conditions in order to find useful configurations for the suppression of electrical breakdowns in TMBi.

2 Electrical breakdown phenomena

The following sections discuss mechanisms of electric breakdown in gases and dielectric liquids.

2.1 Electrical breakdown in gases

Electrical breakdown in gases has significance for many technical applications like the glow discharge in fluorescent tubes, electric arcs in welding or avalanches of charge carriers in a Geiger-Müller detector. In drift detector applications, electrons and ions generated in a neutral gas volume are accelerated by an electric field. As the electric field strength increases, recombination of charge carriers is reduced and more electrons reach the anode contributing to an electric current until all generated charges are collected. When the electrons are accelerated to a higher kinetic energy than the ionization energy of the gas molecules, secondary charge carriers are created, resulting in an avalanche of charged particles. This effect, referred to as Townsend avalanche [20], may trigger an electrical breakdown which is utilized in Geiger-Müller counters but must be avoided for the operation of a proportional drift detector. The Townsend discharge can be described by Paschen's law (Eq. 2.1), where the breakdown voltage U_b depends primarily on the product (pd) of pressure and distance between two parallel electrodes [21]. Without supply of external electrons, i.e. without radioactive source, and for parallel plane electrodes the breakdown voltage can be calculated using

$$U_b = \frac{B \cdot pd}{\ln(A \cdot pd) - \ln\left(\ln\left(1 + \frac{1}{\gamma}\right)\right)}, \quad (2.1)$$

where γ represents the second Townsend coefficient ($\gamma = 0.01$ for stainless steel electrodes) and A and B are empirically determined gas coefficients (see table 1) [22] [23] [24] [25]. For the gases He, Ar, Air, Ne and CO₂, the break down voltages reach a minimum within a pd range between 0.66 mbar · cm and 6 mbar · cm (see figure 1). Left of the Paschen's minima the probability of an avalanche effect is low due to a lack of gas molecules. At higher pd values, the breakdown voltage increases providing stable operating conditions when used in drift detectors. At low pressure near the Paschen's minima a glow discharge may form when charge carriers obtain enough kinetic energy from the electric field to ionize further gas molecules. In an arc discharge it is essentially the emission of electrons from the cathode that contributes to the creation of the DC current. The

Table 1. Constants for the Townsend ionization coefficients based on values from [26].

Gas	A (mbar ⁻¹ · cm ⁻¹)	B (V / (mbar · cm))
He	2	26
Ar	9	135
Air	11	274
Ne	3	751
CO ₂	15	350

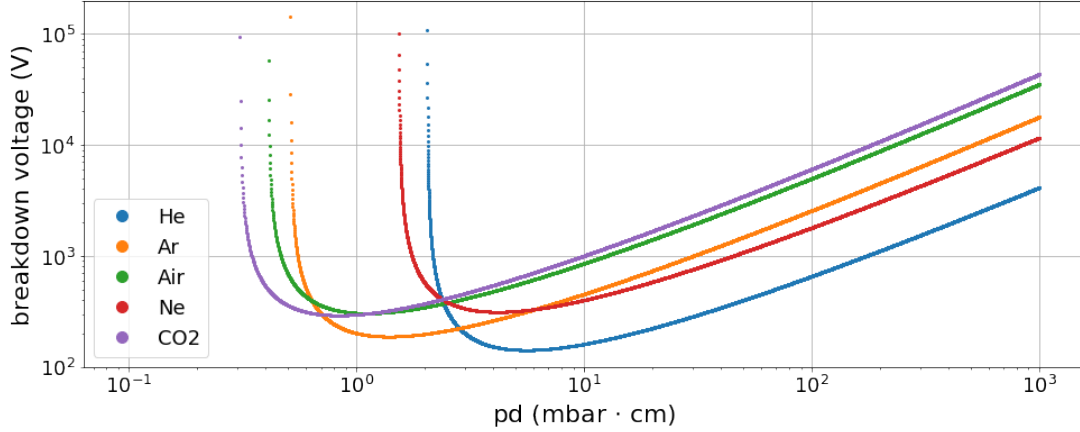


Figure 1. Paschen curves for different gases over a wide range of values for pd , calculated for stainless steel electrodes ($\gamma = 0.01$).

electric current is much higher than in the case of a glow discharge and thus requires a smaller resistance of the external DC circuit [26] [27] [28].

2.2 Electrical breakdown in dielectric liquids

The occurrence of electrical breakdowns in dielectric liquids depends on many factors such as the chemical composition of the liquid and level of impurities, temperature and pressure, irradiation and applied voltages, as well as electrode geometry and surface properties. In the following, only phenomena for DC circuits are considered which are relevant to our experiments [29]. Two common theories exist to describe the initiation of electrical breakdown in dielectric fluids, namely the bubble theory and the direct impact ionization theory [30]. The bubble theory assumes that electrical breakdown begins in a gas bubble near or at an electrode [31]. The generation of such a bubble is the result of an energy injection causing an electron avalanche in the liquid. The formation and size of the bubbles ($\approx \mu\text{m}$) and the live time ($\approx \mu\text{s}$) depends on the operating pressure. The bubbles deform due to Coulomb forces in the direction of the electric field and weaken the liquid's breakdown strength. The elongation of the bubbles leads to an increase in the electric field near the bubble poles. When the electric field reaches a critical value, electrical breakdown starts in the fluid. A Townsend discharge in the bubble can introduce additional electrons in the liquid at the bubble poles, further promoting a breakdown [32][33][34]. With increasing pressure, the bubble volume decreases and the dielectric strength increases [35].

The theory of direct impact ionization provides a description of breakdown effects in liquids without initial bubbles and can be classified into different phases [36]:

1. A trigger phase before breakdown. High electric fields above a few 100 kV/mm, which might occur at micro tips on charged components in the setup, cause local discharges. This will lead to the formation of cavities or volumes with reduced density. The resulting structures form channels in the liquid with a different density than the surrounding medium which in turn leads to an increase in electric current.
2. A phase of expansion of a channel in the liquid. It is called a streamer, which is further divided into positive and negative streamers. Lower electric fields on the magnitude of a few 1 kV/mm are required for generation.
3. A phase of transition to an arc discharge after the streamer short-circuits the electrodes and produces a high current in a low-impedance circuit.

Positive streamers spread out in the direction of the electric field and against the direction of movement of the drift electrons. During the spread the current grows continuously leading to a breakdown quickly after the streamer reaches the cathode [37]. Positive streamers require lower electric fields and are more filamentary than negative streamers and pose a higher risk for technical applications [38] [39]. Negative streamers spread out against the direction of the electric field and in the direction of movement of the drift electrons. They are less filamentary than positive streamers [37]. The current during growth consists of successive fast pulses. In contrast to positive streamers, the influence of pressure on the spread of negative streamers is stronger [40] [41].

The influence of pressure on dielectric strength is evident both in the formation of bubbles and in the initialization of direct impact ionization. With increasing pressure, the dielectric strength increases. Correspondingly, the number and amplitude of the current pulses, as well as the shape and length of the streamers, decrease [37] [40] [42] [43]. A minimum dielectric strength is reached near the boiling point of the liquid or near the boiling points of residual gas inclusions [44] [45]. In studies with point-plane geometries, the transition to a streamer phenomenon is observed as a result of fast and repeated energy injection by electron avalanches, which correlates with the generation of successive bubbles [35]. The dielectric strength depends also on the nature and quantity of impurities in the liquid [37]. Even small contaminations can lead to an increased current and a reduction in breakdown voltage. In tests with liquid argon, the breakdown voltage was a factor ≈ 1.5 higher for levels of oxygen impurities above 0.2 ppm than for concentrations below 1.8 ppb [46].

Electrical breakdowns must be avoided when operating a drift detector and even more importantly when using a pyrophoric liquid such as TMBi. In the experiments described in this paper, conditions that favor or prevent electrical breakdowns in TMBi have been investigated and methods for stable operation are discussed.

2.3 Electrical breakdown behavior of TMBi

In an electrical breakdown (in the gas phase), TMBi decomposes via an exothermic redox reaction into lower methyl bismuth species including $(\text{CH}_3)\text{Bi}$ and $(\text{CH}_3)_2\text{Bi}$ [47]. Similar decomposition products are generated during the electron bombardment in the ion source of a quadrupole mass

spectrometer (PrismaPro QMG 250 M3, Pfeiffer Vacuum GmbH, Germany) (see figure 2). The difference between the bond enthalpies of the products and reactants is converted into heat. If the temperature becomes sufficiently high, TMBi decomposes in a chain reaction [48][49]. If oxygen comes into contact with the TMBi, carbon, or hydrocarbon residues during the redox reaction, this can lead to combustion (e.g. into Bi_2O_3 , CO_2 and water) with the formation of flames [50]. Both effects, decomposition and combustion, will lead to a sudden volume expansion and therefore present a safety hazard.

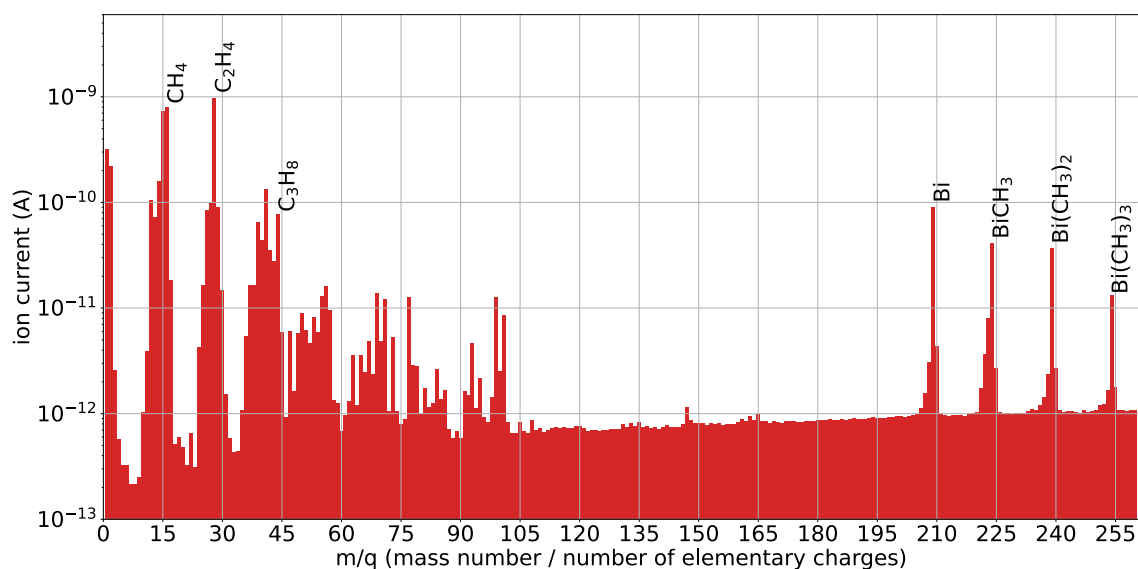


Figure 2. Spectrum of decomposition products of trimethyl bismuth taken with a quadrupole mass filter. The main components at mass numbers above 200 are Bi (209 amu), $\text{Bi}(\text{CH}_3)$ (224 amu), $\text{Bi}(\text{CH}_3)_2$ (239 amu), and $\text{Bi}(\text{CH}_3)_3$ (254 amu). The various hydrocarbon compounds like ethene C_2H_4 (28 amu), ethane C_2H_6 (30 amu), and propane C_3H_8 (44 amu) appear at lower mass numbers.

3 Setup for breakdown experiments

To study the behaviour of TMBi under the influence of different electric fields and different environmental conditions, the liquid was filled into a small glass vessel with electrodes introduced on both ends and hermetically sealed inside a large glass cylinder (see figure 3). The sample vessel (1) was manufactured by our local glassblower with an opening on top and a volume of $V \approx 1.5$ ml. Two stainless steel rods (2) with electropolished front faces and a diameter of 2 mm were mounted via PTFE inlets (3) on both ends of the glass vessel, serving as electrodes. They had a distance of 2 mm and were contacted using spring-loaded clamps (4). Vessel and contacts were mounted on a plastic base-plate (5) which was arranged in an outer glass cylinder (6) (Lenz Laborglas GmbH & Co.KG, Wertheim, Germany) with a conical ground joint (45/40) and a head closure (7). A high-voltage cable (8) was fed through a rubber sealed entry cap fixed with a twist lock (9). A one-way connecting stopcock (10) (Gebr. Rettberg GmbH, Göttingen, Germany) was connected to a water jet pump (BRAND GMBH + CO KG, Wertheim, Germany) to achieve pressures down to $p \approx 20$ mbar inside the cylinder. High voltage was supplied to the electrodes using an iseg NHQ 224M HV module

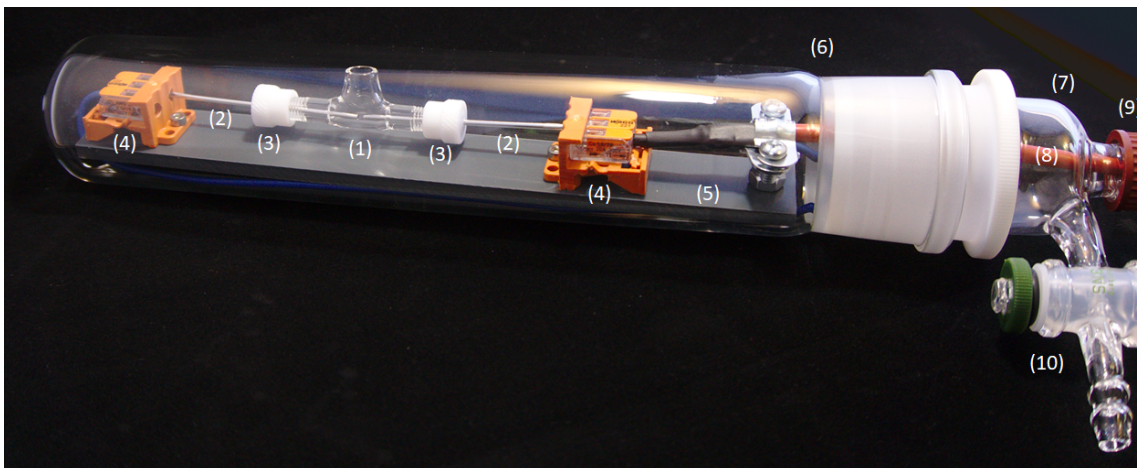


Figure 3. Experimental setup with sample glass container (1) in which high voltage can be applied to the TMBi liquid by two electropolished stainless steel electrodes (distance of 2 mm). The sample container is sealed by an outer glass cylinder (6) which can be evacuated using a water jet pump.

(iseg Spezialelektronik GmbH, Radeberg, Germany) offering an adjustable voltage up to 4000 V and an integrated display of the current with a resolution of 1 nA. All experiments were performed inside a laboratory fume hood with the setup arranged behind a thick perspex window for safety.

A high speed video camera (acA2000-165um, Basler AG, Ahrensburg, Germany, max. 165 frames per second) was placed in front of the experiment to monitor the test cell. In order to estimate the pressure generated by the water jet pump, a measurement was carried out beforehand in a vacuum system with a comparable volume to the test set-up. The pressure measured using a dedicated sensor (Pirani Gauge FRG-700, Agilent Technologies, Santa Clara, CA, USA) dropped exponentially with time reaching a minimum of 20 mbar after 160 seconds.

4 Measurement results

The following sections describe a series of experiments using TMBi under different atmospheres and at different ambient pressures. The tests were prepared by filling TMBi into the sample container and sealing it inside the glass cylinder described in section 3 under a clean argon atmosphere inside a glove box. The closed cylinder was then transferred to the laboratory hood and connected to the water jet pump and the high voltage supply. The negative high voltage terminal of the power supply was connected to the cathode and the anode was connected to ground potential. In experiments 1 - 3, the seal of the high voltage cable entry into the cylinder turned out to be leaky which allowed to study effects of oxygen contamination at different pressures. In experiments 4 to 5, the high-voltage cable feed-through was made airtight and additionally the glass cylinder was placed into a second container filled with argon to prevent entry of oxygen during the evacuation phase.

4.1 Experiment 1: 1 bar argon atmosphere and oxygen contamination.

In the first test, the TMBi filled vessel was kept inside the argon filled cylinder under atmospheric pressure while applying increasingly negative voltages to the cathode. The voltage was increased

in 500 V steps up to 4000 V (maximum voltage of the HV supply) in 1 minute intervals. Starting at a voltage of 2000 V visible movements in the liquid with floating particles moving close to the electrodes were observed. The particles are believed to be reaction products of TMBi and oxygen. After increasing the voltage further to 3000 V, the measured current started to oscillate between 0 nA and 3 nA over time intervals of a few seconds. At even higher voltages of 3500 V and 4000 V the fluctuation amplitudes increased to 4 nA and 6 nA, respectively. Figure 4 shows on the upper panel a photograph of the TMBi filled sample vessel during the test.

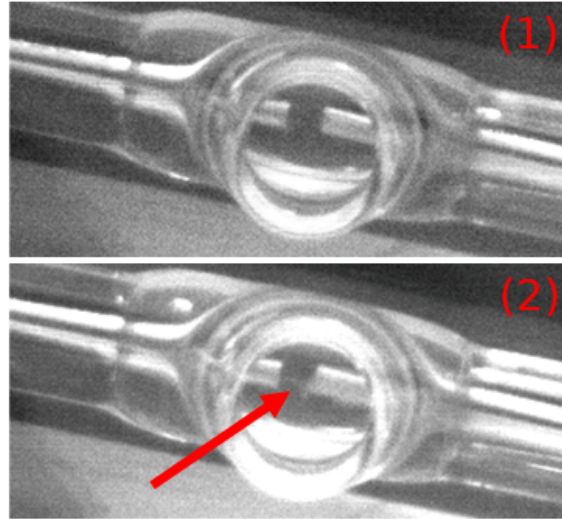


Figure 4. Upper panel: At a pressure of 1 bar (experiment 1) no discharges appeared up to 4000 V. Lower panel: In experiment 2, a discharge channel formed between the electrodes at 2000 V.

4.2 Experiment 2: vapor pressure (40 mbar) and oxygen contamination.

For the second test, the voltage was turned down and the outer cylinder was evacuated using the water jet pump until the TMBi started to boil. At that point, the valve to the pump was closed and the pressure inside the cylinder increased to 40 mbar corresponding to the vapor pressure of TMBi at room temperature [51][52]. While increasing the voltage from 0 V to 4000 V in 500 V steps at this lower pressure, the current oscillations already started at 500 V where we observed fluctuations up to 2 nA. These fluctuations increased to 4 nA at 1000 V and up to 5 nA at 1500 V. At an applied voltage of 2000 V the current initially stabilized at 8 nA. After another minute at the same voltage, the current increased to 11 nA and a discharge channel formed between the electrodes (see figure 4, lower panel). The current then increased from 20 nA to 23 nA at an applied voltage of 2500 V. Increasing the voltage to 3000 V raised the current up to 41 nA. At 3500 V, the surface of the liquid started to move and at 4000 V the current increased up to 182 nA where the experiment was aborted (see figure 5).

4.3 Experiment 3: low pressure (< 40 mbar) and oxygen contamination

In the third test, the pressure inside the cylinder was lowered to < 40 mbar by continuous pumping while applying a voltage of -4000 V. Due to the leak at the HV cable feedthrough, additional

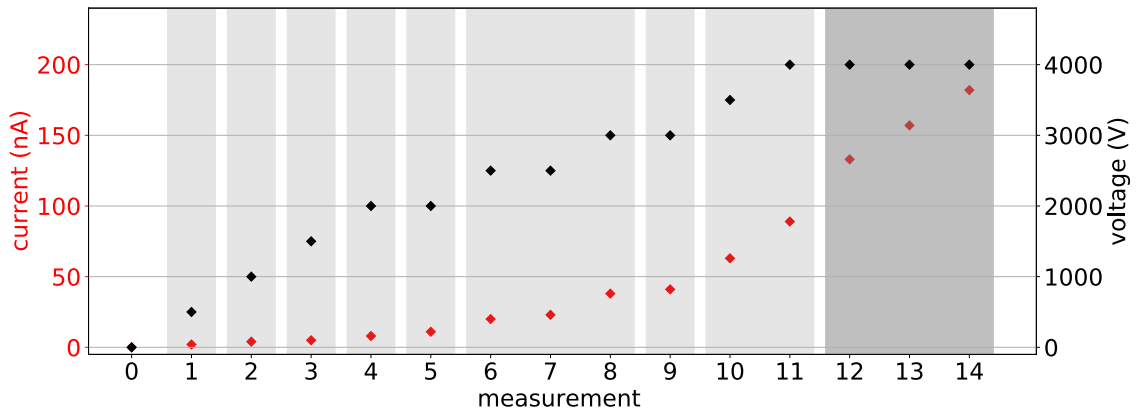


Figure 5. In experiment 2, the current increased as a function of the applied voltage (light grey equals to 1 min, dark grey to 10 min time scales). At 4000 V, the current increased continuously and the test was stopped.

oxygen entered into the cylinder and reacted with the TMBi causing a milky discoloration (see figure 6, left photo). Within the first 2 minutes, the current increased from 82 nA to 100 nA. After

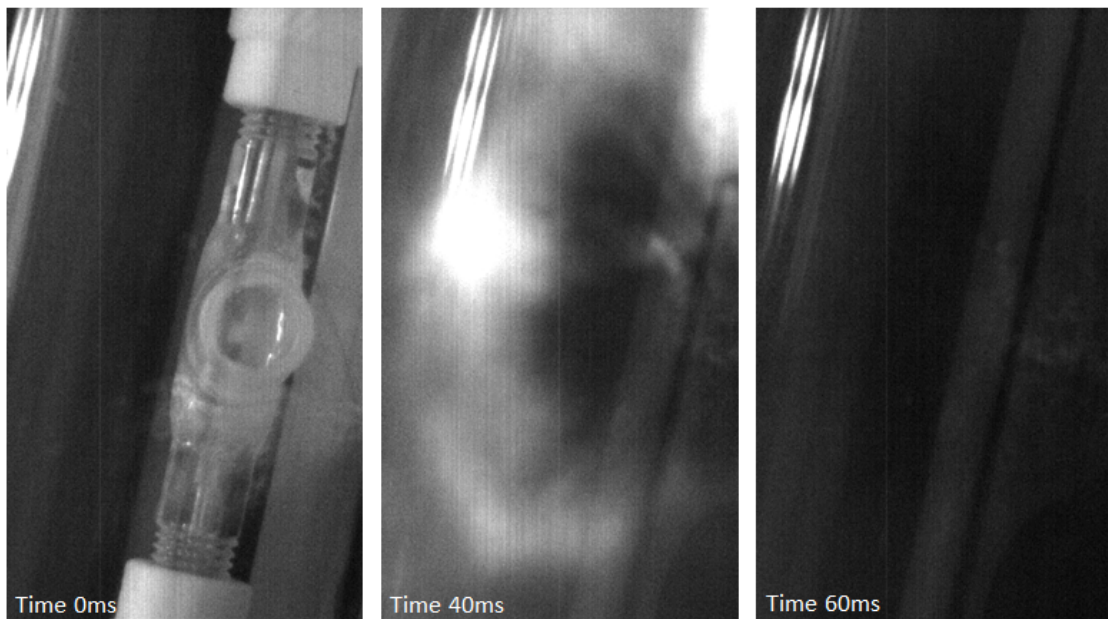


Figure 6. Photos of the sample cell before (left), during (middle) and after (right) the TMBi combustion. The milky discoloration of the TMBi described in the text is visible on the left photo. The combustion completely blackened the outer cylinder (right photo).

3 minutes of pumping the TMBi started to boil. The current increased to 3.8 μ A followed by an explosion of the TMBi which decomposed completely in the process (see figure 6, middle and right photographs).

4.4 Experiment 4: low pressure argon atmosphere

For the second round of measurements a new sample vessel was constructed, where the TMBi inlet is not positioned directly above the electrode gap, but on one side and at an angle. This allows to perform tests with an upright geometry where one electrode is submerged in the liquid and the other electrode positioned in the gas phase (see figure 8, right photograph). An additional bulge above the electrode gap allows to observe the amount of gaseous TMBi formed in tests where the vessel is operated horizontally. As mentioned above, the leak observed in the previous measurements was fixed and, as an additional safeguard, the cylinder was placed in an argon filled containment to ensure that no oxygen can enter the sample vessel.

At the beginning of the measurement, the electrodes were completely covered with TMBi. The water jet pump was operated for 100 seconds reaching a pressure ≤ 100 mbar. Subsequently, the voltage was increased in steps of 500 V in 1 minute intervals up to a maximum of 4000 V. Except for a temporary increase to 0.6 nA at 4000 V the measured current remained at 0 nA.

To further lower the pressure, the water jet pump was operated for an additional 115 seconds and the TMBi filling level decreased due to evaporation until the electrodes were no longer completely covered (see figure 7, first photo). The voltage, which was turned off before pumping, was increased

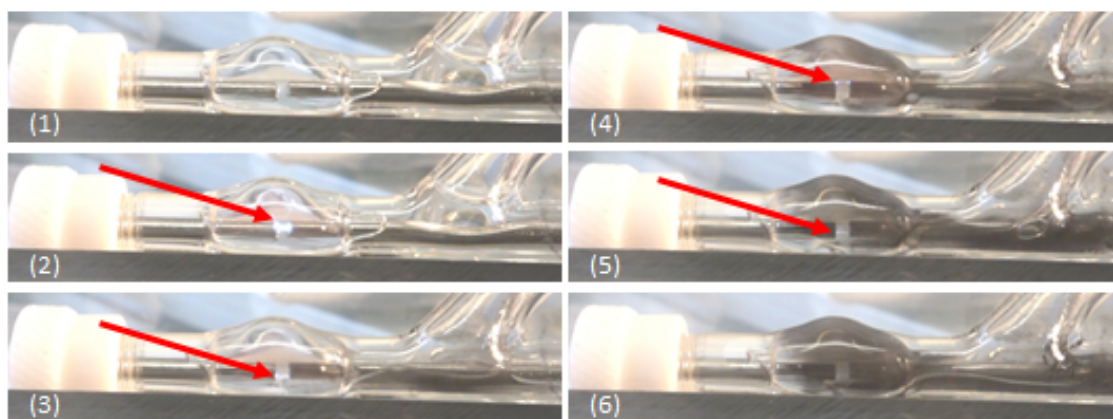


Figure 7. Experiment 4: TMBi in argon atmosphere at vapor pressures down to 20 mbar. At 4000 V, electrical breakdowns occurred between the electrodes leading to a decomposition of TMBi. The images were recorded in time from top left to bottom right over a one minute interval.

again step by step. At 3000 V the current increased to 0.2 nA for a few seconds, decreased again and remained at 0 nA for the rest of the measurement.

Finally, the water jet pump was operated permanently while keeping the voltage at 4000 V. After ca. 2 minutes the liquid started to boil and electrical flash-overs occurred in the gas phase above the liquid. Parts of the TMBi decomposed and formed black residues on the glass surfaces of the sample container (see photographs 4-6 in figure 7). However, due to the absence of oxygen, the liquid did not spontaneously explode.

4.5 Experiment 5: 1 bar argon atmosphere

The last series of measurements was again performed with different TMBi levels in the sample vessel but this time keeping a 1 bar argon atmosphere in the cylinder at all times. Tests were



Figure 8. Experiment 5: Upper left: setup with electrodes completely covered with liquid. Lower left: reduced filling level with electrodes half covered with TMBi. Right: rotated setup with the lower electrode submerged in TMBi and the upper electrode in the gas phase. An argon pressure of 1 bar was present throughout the tests.

performed with completely covered electrodes, with partially covered electrodes and with the container in a vertical orientation, where the anode was submerged in TMBi while the cathode was positioned in the gas phase (see figure 8). The current was measured while applying voltages up to 4000 V. Besides the current, the liquid was monitored for fluid movements, the formation of bubbles, discharge channels or other disturbances. Neither during the initial ramping nor during prolonged measurements exceeding 30 minutes at 4000 V, any changes were observed in the liquid or electric current. Experiments with a 1 bar argon atmosphere were repeated several times with similar findings and without any breakdown occurrences, giving us confidence that this mode of operation indeed allows for stable operation of TMBi filled measurement cells.

5 Conclusion

The objective of this study was to investigate the behaviour of TMBi under different ambient conditions and different electric field strengths to find conditions for stable and safe operation of a liquid-based ionization detector. For that purpose a test setup containing a TMBi filled sample cell was constructed that allowed to work under an argon atmosphere at different pressures while applying varying electric fields to the liquid. During the first measurements an oxygen contamination was present inside the test cylinder due to a leaky feedthrough. This actually allowed us to study the effect of an electro-negative contamination in the liquid on the high-voltage stability.

Our findings may be summarized as follows: Under argon atmospheres at 1 bar pressure we did not observe breakdowns of the electrical potential in our measurement cell up to maximum field strengths of 20 kV/cm. The presence of oxygen contaminations in the first series of measurements

did, however, led to fluctuating currents in the nA range, which were not observed under a completely pure argon atmosphere.

Lowering the pressure to about 40 mbar, corresponding to the TMBi vapor pressure at room temperature, lead to the formation of a discharge channel in the liquid and a steady increase in the current in the presence of oxygen contaminations (the measurement was stopped at a current of 182 nA). Further reduction of pressure caused the liquid to boil and, in the presence of oxygen, led to a spontaneous combustion of the TMBi.

With the improved setup, allowing measurements under a pure argon atmosphere, no continuous current was observed even when the electrodes were not completely covered in TMBi. At pressures below the boiling point the TMBi started to decompose at the applied field of 20 kV/cm, but without the explosive character observed earlier. The presence of 1 bar argon prevented the liquid from boiling at room temperature. A slight overpressure compared to the ambient air pressure also minimizes the instrument's risk of oxygen ingress. Although an even higher pressure would result in a higher breakdown voltage, it would probably be incompatible with many vacuum components.

If the electrodes are not completely immersed in the liquid, the breakdown mechanisms in gases will come into effect causing a reduction of the allowable field strength (see Paschen's curve in figure 1). Also, our tests show that electro-negative contaminations in the liquid have an important and detrimental effect on the electric stability of the medium.

When going to pressures close to the vapor pressure of the liquid, small additional pressure or temperature changes will cause the liquid to boil and will change the conditions for an electrical breakdown in the medium. In a liquid argon study, the breakdown voltage decreased from > 100 kV/cm to 40 kV/cm when the liquid started to boil [53]. Thus, special care has to be taken to avoid such situations.

We conclude that in the presence of a pure argon atmosphere at 1 bar pressure, a detector with plane-parallel electrodes completely covered in a purified dielectric liquid such as TMBi remains stable against electrical breakdown at least up to electric field strengths of 20 kV/cm, which we had available during our measurements.

Acknowledgments

We would like to thank Deutsche Forschungsgemeinschaft (DFG), project numbers WE 1843/8-1 and SCHA 1447/3-1, French national research agency (ANR), project number ANR-18-CE92-0012-01, and Axel Buß for providing the photography in figure 3.

References

- [1] H. Klages, W. Apel, K. Bekk, E. Bollmann, H. Bozdog, I. Brancus et al., The cascade experiment, *Nuclear Physics B-Proceedings Supplements* **52** (1997) 92.
- [2] Y. Xing, M. Abaline, S. Acounis, N. Beaupère, J. Beney, J. Bert et al., Xemis: Liquid xenon compton camera for 3 γ imaging, in *International conference on Technology and Instrumentation in Particle Physics*, pp. 154–158, Springer, 2017.
- [3] L. G. Manzano, J. Abaline, S. Acounis, N. Beaupère, J. Beney, J. Bert et al., Xemis2: A liquid xenon detector for small animal medical imaging, *Nuclear Instruments and Methods in Physics Research Section A: Accelerators, Spectrometers, Detectors and Associated Equipment* **912** (2018) 329.

- [4] E. Aprile and T. Doke, Liquid xenon detectors for particle physics and astrophysics, Reviews of Modern Physics **82** (2010) 2053.
- [5] E. Aprile, J. Aalbers, F. Agostini, M. Alfonsi, L. Althueser, F. Amaro et al., Projected wimp sensitivity of the xenonnT dark matter experiment, Journal of Cosmology and Astroparticle Physics **2020** (2020) 031.
- [6] E. Aprile, J. Aalbers, F. Agostini, S. A. Maouloud, M. Alfonsi, L. Althueser et al., Search for coherent elastic scattering of solar $\bar{\nu}_e$ neutrinos in the xenonT dark matter experiment, Physical Review Letters **126** (2021) 091301.
- [7] Y. Meng, Z. Wang, Y. Tao, A. Abdurkerim, Z. Bo, W. Chen et al., Dark matter search results from the pandax-4t commissioning run, Physical Review Letters **127** (2021) 261802.
- [8] D. Akerib, C. Akerlof, D. Y. Akimov, A. Alqahtani, S. Alsum, T. Anderson et al., The lux-zeplin (Lz) experiment, Nuclear Instruments and Methods in Physics Research Section A: Accelerators, Spectrometers, Detectors and Associated Equipment **953** (2020) 163047.
- [9] J. Aalbers, F. Agostini, M. Alfonsi, F. Amaro, C. AMSLER, E. Aprile et al., Darwin: towards the ultimate dark matter detector, Journal of Cosmology and Astroparticle Physics **2016** (2016) 017.
- [10] G. Adhikari, S. Al Kharusi, E. Angelico, G. Anton, I. Arnquist, I. Badhrees et al., nexo: neutrinoless double beta decay search beyond 1028 year half-life sensitivity, Journal of Physics G: Nuclear and Particle Physics **49** (2021) 015104.
- [11] C. Adams, V. Álvarez, L. Arazi, I. Arnquist, C. Azevedo, K. Bailey et al., Sensitivity of a tonne-scale next detector for neutrinoless double-beta decay searches, Journal of High Energy Physics **2021** (2021) 1.
- [12] E. Aprile, J. Aalbers, F. Agostini, M. Alfonsi, F. Amaro, M. Anthony et al., The xenonT dark matter experiment, The European Physical Journal C **77** (2017) 1.
- [13] L. G. Manzano, S. Bassetto, N. Beaupere, P. Briend, T. Carlier, M. Cherel et al., Xemis: A liquid xenon detector for medical imaging, Nuclear Instruments and Methods in Physics Research Section A: Accelerators, Spectrometers, Detectors and Associated Equipment **787** (2015) 89.
- [14] P. Ferrario, P. collaboration et al., Status and perspectives of the petalo project, Journal of Instrumentation **17** (2022) C01057.
- [15] D. Yvon, J.-P. Renault, G. Tauzin, P. Verrecchia, C. Flouzat, S. Sharyy et al., Calipso: An novel detector concept for pet imaging, IEEE Transactions on Nuclear Science **61** (2014) 60.
- [16] M. Farradèche, G. Tauzin, J.-P. Mols, J. Bard, J. Dognon, C. Weinheimer et al., Ionization parameters of trimethylbismuth for high-energy photon detection, Nuclear Instruments and Methods in Physics Research Section A: Accelerators, Spectrometers, Detectors and Associated Equipment **958** (2020) 162646.
- [17] G. Freeman and J.-P. Dodelet, On onsager's charge recombination theory applied to liquid alkanes, International Journal for Radiation Physics and Chemistry **5** (1973) 371.
- [18] L. Onsager, Initial recombination of ions, Physical Review **54** (1938) 554.
- [19] M. Farradèche, Chambre d'ionisation liquide détecteur de photons γ pour l'imagerie TEP, Ph.D. thesis, Université Paris Saclay (COMUE), 2019.
- [20] J. Townsend, The conductivity produced in gases by the motion of negatively-charged ions, Nature **62** (1900) 340.

- [21] M. M. Pejovic, G. S. Ristic and J. P. Karamarkovic, Electrical breakdown in low pressure gases, *Journal of Physics D: Applied Physics* **35** (2002) R91.
- [22] K. Burm, Calculation of the townsend discharge coefficients and the paschen curve coefficients, *Contributions to Plasma Physics* **47** (2007) 177.
- [23] A. Von Engel, Ionized gases. American Institute of Physics, Melville, NY, 1 ed., 1965.
- [24] L. Norman, K. Silva, B. Jones, A. McDonald, M. Tiscareno and K. Woodruff, Dielectric strength of noble and quenched gases for high pressure time projection chambers, *The European Physical Journal C* **82** (2022) 1.
- [25] R. Massarczyk, P. Chu, C. Dugger, S. Elliott, K. Rielage and W. Xu, Paschen's law studies in cold gases, *Journal of Instrumentation* **12** (2017) P06019.
- [26] Y. P. Raizer and J. E. Allen, Gas discharge physics. Springer, Heidelberg, Germany, 1 ed., 1991.
- [27] H. Kurt and B. Salamov, Behaviour of current in a planar gas discharge system with a large-diameter semiconductor cathode, *Journal of Physics D: Applied Physics* **36** (2003) 1987.
- [28] V. Lisovskii and S. Yakovin, A modified paschen law for the initiation of a dc glow discharge in inert gases, *Technical Physics* **45** (2000) 727.
- [29] W. Schmidt, Liquid state electronics of insulating liquids. CRC Press, Boca Raton, Florida, 1997.
- [30] P. Wedin, Electrical breakdown in dielectric liquids-a short overview, *IEEE Electrical Insulation Magazine* **30** (2014) 20.
- [31] A. H. Sharbaugh, J. C. Devins and S. J. Rzed, Progress in the field of electric breakdown in dielectric liquids, *IEEE Transactions on Electrical Insulation* **EI-13** (1978) 249.
- [32] S. Korobeynikov and Y. N. Sinikh, Bubbles and breakdown of liquid dielectrics, in Conference Record of the 1998 IEEE International Symposium on Electrical Insulation (Cat. No. 98CH36239), vol. 2, pp. 603–606, IEEE, 1998.
- [33] I. Alexeff, M. Pace, T. Blalock and A. Wintenberg, Possible models for the earliest prebreakdown events in dc stressed hexane, in 10th International Conference on Conduction and Breakdown in Dielectric Liquids, pp. 387–391, IEEE, 1990.
- [34] H. Jones and E. Kunhardt, Development of pulsed dielectric breakdown in liquids, *Journal of Physics D: Applied Physics* **28** (1995) 178.
- [35] R. Kattan, A. Denat and O. Lesaint, Generation, growth, and collapse of vapor bubbles in hydrocarbon liquids under a high divergent electric field, *Journal of Applied Physics* **66** (1989) 4062.
- [36] A. Denat, Conduction and breakdown initiation in dielectric liquids, in 2011 IEEE International Conference on Dielectric Liquids, pp. 1–11, IEEE, 2011.
- [37] J. C. Devins, S. J. Rzed and R. J. Schwabe, Breakdown and prebreakdown phenomena in liquids, *Journal of Applied Physics* **52** (1981) 4531.
- [38] O. Lesaint and P. Gournay, On the gaseous nature of positive filamentary streamers in hydrocarbon liquids. i: Influence of the hydrostatic pressure on the propagation, *Journal of Physics D: Applied Physics* **27** (1994) 2111.
- [39] R. Tobazcon, Prebreakdown phenomena in dielectric liquids, *IEEE Transactions on Dielectrics and Electrical Insulation* **1** (1994) 1132.
- [40] A. Beroual, M. Zahn, A. Badent, K. Kist, A. Schwabe, H. Yamashita et al., Propagation and structure of streamers in liquid dielectrics, *IEEE Electrical Insulation Magazine* **14** (1998) 6.

- [41] A. Denat, High field conduction and prebreakdown phenomena in dielectric liquids, IEEE Transactions on Dielectrics and Electrical Insulation **13** (2006) 518.
- [42] P. K. Watson and A. H. Sharbaugh, High-field conduction currents in liquid n-hexane under microsecond pulse conditions, Journal of The Electrochemical Society **107** (1960) 516.
- [43] A. Beroual and R. Tobazeon, Effects of hydrostatic pressure on the prebreakdown phenomena in dielectric liquids, in Conference on Electrical Insulation & Dielectric Phenomena-Annual Report 1985, pp. 44–49, IEEE, 1985.
- [44] F. Clark, The electrical breakdown of liquid dielectrics, Journal of the Franklin Institute **216** (1933) 429.
- [45] K. C. Koo and J. B. Higham, The effects of hydrostatic pressure, temperature, and voltage duration on the electric strengths of hydrocarbon liquids, Journal of The Electrochemical Society **108** (1961) 522.
- [46] R. Acciarri, B. Carls, C. James, B. Johnson, H. Jostlein, S. Lockwitz et al., Liquid argon dielectric breakdown studies with the microboone purification system, Journal of Instrumentation **9** (2014) P11001.
- [47] O. P. Strausz, J. Connor and P. J. Young, Flash photolysis of trimethylantimony and trimethylbismuth and the quenching of excited antimony and bismuth atoms, Journal of the American Chemical Society **93** (1971) 822.
- [48] D. R. Lide, CRC handbook of Chemistry and Physics, vol. 85. CRC press, Boca Raton, Florida, 2004.
- [49] E. Riedel and C. Janiak, Anorganische Chemie. de Gruyter, Berlin, Germany, 10 ed., 2022.
- [50] L. Long and J. Sackman, The heat of formation of bismuth trimethyl, Transactions of the Faraday Society **50** (1954) 1177.
- [51] E. Amberger, Hydride des wismuts, Chemische Berichte **94** (1961) 1447.
- [52] P. Morávek, M. Fulem, J. Pangrác, E. Hulcius and K. Růžicka, Vapor pressures of dimethylcadmium, trimethylbismuth, and tris (dimethylamino) antimony, Fluid Phase Equilibria **360** (2013) 106.
- [53] F. Bay, C. Cantini, S. Murphy, F. Resnati, A. Rubbia, F. Sergiampietri et al., Evidence of electric breakdown induced by bubbles in liquid argon, arXiv preprint arXiv:1401.2777 (2014) .